AGU PUBLICATIONS

Geophysical Research Letters

Supporting Information for

A Global Survey of Lithospheric Flexure at Steep-Sided Domical Volcanoes on Venus Reveals Intermediate Elastic Thicknesses

M. E. Borrelli[1], J. G. O'Rourke[1], S. E. Smrekar[2], C. M. Ostberg[3]

[1]Arizona State University, School of Earth and Space Exploration, Tempe, AZ.

[2]Jet Propulsion Laboratory, California Institute of Technology, Pasadena, CA.

[3]University of California, Department of Earth and Planetary Sciences, Riverside, CA.

Contents of this file

Tables S1 to S3, Figure S1

Additional Supporting Information (Files uploaded separately)

Captions for Datasets S1 to S2

Introduction

This Supporting Information includes tables that complement the main text, along with datasets that could be used to reproduce our results. All topographic profiles were extracted from the Magellan global topographic data record (GTDR) and, where available, stereo-derived digital elevation maps using JMARS.

Table S1
Values of constants used in curve-fitting functions and calculations, which were taken from Johnson & Sandwell (1994) except the rheological laws for dry olivine and diabase are from McNutt (1984) and Mackwell et al. (1998), respectively.

Constant	Definition	Value	Units
g	Gravitational acceleration at the surface of Venus	8.87	m/s^2
E	Young's modulus	100	GPa
$\Delta\rho$	Density contrast across the lithosphere	3300	kg/m^3
ν	Poisson's ratio	0.25	
k_C	Thermal conductivity of the lithosphere	4	W/m/K
T_C	Critical temperature for dry olivine (above which the ductile strength is ≤50 MPa)	1013	K
T_C	Critical temperature for dry diabase (Columbia)	1013	K
T_C	Critical temperature for dry diabase (Maryland)	961	K
T_S	Surface temperature on Venus	740	K

Table S2

List of all domes with at least one topographic profile amenable to a flexural interpretation. From left to right, the first four columns show the index number, diameter, longitude, and latitude of each dome. Mechanical thicknesses (h_e) and surface heat flows (F_S) were derived using yield stress envelopes for two types of dry diabase (Mackwell et al., 1998).

				Maryland		Columbia	
Dome	**Dia. (km)**	**Lon (°)**	**Lat (°)**	**h_m (km)**	**F_s (mW/m^2)**	**h_m (km)**	**F_s (mW/m^2)**
1	35	151.0	-3.0	38.1 ± 1.5	28.7 ± 1.1	38.1 ± 1.5	28.7 ± 1.1
2	40	80.0	-26.0	5.3 ± 0.1	279.7 ± 13.9	5.3 ± 0.1	279.0 ± 13.5
5	30	63.0	28.0	17.3 ± 1.1	63.9 ± 3.7	17.3 ± 1.1	63.9 ± 3.6
7	30	79.0	42.5	20.3 ± 0.5	61.3 ± 1.6	20.3 ± 0.5	61.3 ± 1.6
13	25	68.5	28.0	16.3 ± 0.5	68.1 ± 8.4	16.2 ± 2.0	68.3 ± 8.5
16	30	66.0	37.5	24.3 ±1.3	45.0 ± 2.4	24.4 ± 1.3	44.9 ± 2.4
20	20	85.0	57.0	29.7 ± 1.4	36.8 ± 2.7	29.7 ± 1.4	36.8 ± 1.7
21	25	97.5	50.0	33.6 ± 3.4	32.9 ± 3.4	33.5 ± 3.4	32.9 ± 3.4
22	25	342.0	48.0	41.7 ± 2.8	26.3 ± 1.8	41.8 ± 2.8	26.3 ± 1.8
26	50	311.5	34.0	10.0 ± 0.5	109.3 ± 5.9	10.0 ± 0.6	109.2 ± 6.2
32	20	314.0	25.0	17.6 ± 0.9	62.3 ± 3.3	17.6 ± 0.9	62.4 ± 3.3
51	20	247.0	-12.5	5.1 ± 0.1	216.3 ± 5.2	5.1 ± 0.1	216.3 ± 5.2
64	30	264.0	-35.0	5.8 ± 0.3	190.0 ± 9.1	5.8 ± 0.3	190.1 ± 9.1
75 a	25	162.0	-58.0	20.7 ± 0.6	91.1 ± 4.8	20.1 ± 0.6	91.1 ± 4.7
75 b	25	162.0	-58.0	15.0 ± 0.4	104.0 ± 3.6	15.0 ± 0.4	104.0 ± 3.6

Table S3
Results from each individual profile for steep-sided domes with multiple profiles that were amenable to flexural interpretation.

				Dry Olivine		Maryland Diabase		Columbia Diabase	
Dome	**Profile**	**Axi. h_e (km)**	**Cart. h_e (km)**	**h_m (km)**	**F_s (mW/m^2)**	**h_m (km)**	**F_s (mW/m^2)**	**h_m (km)**	**F_s (mW/m^2)**
2	1	5.2 ± 0.1	4.6 ± 0.2	6.3 ± 0.1	173.6 ± 3.0	3.0 ± 6.3	173.6 ± 3.0	6.4 ± 0.1	173.6 ± 3.0
2	2	4.7 ± 1.0	3.0 ± 0.2	5.3 ± 0.9	210.9 ± 38.5	40.5 ± 5.3	211.4 ± 40.2	5.3 ± ± 0.9	211.9 ± 40.5
2	3	9.9 ± 0.5	7.6 ± 0.6	11.5 ± 0.4	94.8 ± 3.3	3.4 ± 11.5	94.8 ± 3.4	11.5 ± 0.4	94.9 ± 3.4
2	4	2.5 ± 0.2	2.1 ± 0.1	3.2 ± 0.2	339.4 ± 17.2	17.5 ± 3.2	338.9 ± 17.3	3.2 ± 0.2	339.1 ± 17.5
2	5	1.3 ± 0.3	1.2 ± 0.2	2.1 ± 0.3	547.6 ± 99.4	100.8 ± 2.1	545.3 ± 97.1	2 ± 0.3	549.4 ± 100.8
2	6	2.3 ± 0.1	1.5 ± 0.1	3.3 ± 0.1	334.5 ± 10.4	10.6 ± 3.3	334.1 ± 10.4	3.3 ± 0.1	334.7 ± 10.6
2	7	2.2 ± 0.1	1.9 ± 0.1	2.8 ± 0.1	394.6 ± 8.9	9.0 ± 2.8	394.4 ± 9.0	2.8 ± 0.1	394.7 ± 9.0
2	8	7.4 ± 0.4	4.5 ± 0.3	7.9 ± 0.4	139.5 ± 6.3	6.3 ± 7.8	139.5 ± 6.3	7.9 ± 0.4	139.4 ± 6.3
5	1	18.3 ± 1.8	23.3 ± 1.9	18.7 ± 1.8	59.0 ± 5.7	5.6 ± 18.7	59.0 ± 5.7	18.7 ± 1.8	58.8 ± 5.6
5	2	15.2 ± 1.1	16.4 ± 0.8	15.9 ± 1.1	69.1 ± 4.6	4.7 ± 15.9	69.0 ± 4.6	15.9 ± 1.1	69.1 ± 4.7
7	4	24.9 ± 1.0	26.8 ± 1.0	27.3 ± 0.8	40.1 ± 1.2	1.2 ± 27.2	40.1 ± 1.3	27.3 ± 0.8	40.1 ± 2.1
7	5	8.9 ± 0.6	7.7 ± 0.6	13.3 ± 0.5	82.5 ± 3.0	3.0 ± 13.3	82.5 ± 3.0	13.2 ± 0.5	82.6 ± 3.0
75	1	26.5 ± 0.9	30.3 ± 1.0	27.6 ± 0.9	39.6 ± 1.2	1.2 ± 27.6	39.6 ± 1.2	27.6 ± 0.8	39.6 ± 1.2
75	2	27.6 ± 1.6	31.9 ± 1.6	28.9 ± 1.4	37.9 ± 1.9	1.8 ± 29.0	37.8 ± 1.9	28.9 ± 1.4	37.9 ± 1.8
75	3	15.5 ± 0.7	20.0 ± 0.7	16.6 ± 0.6	66.0 ± 2.3	2.3 ± 16.6	65.9 ± 2.3	16.6 ± 0.6	66.0 ± 2.3
75	4	28.3 ± 1.1	29.3 ± 0.9	29.4 ± 1.1	37.3 ± 1.3	1.3 ± 29.3	37.3 ± 1.3	29.3 ± 1.1	37.3 ± 1.3
75	5	6.7 ± 0.7	8.8 ± 0.8	7.5 ± 0.6	147.2 ± 12.5	12.5 ± 7.5	147.6 ± 12.4	7.5 ± 0.6	147.6 ± 12.5
75	6	5.6 ± 0.3	6.8 ± 0.4	6.6 ± 0.3	165.1 ± 6.4	6.5 ± 6.6	165.1 ± 6.5	6.6 ± 0.3	165.3 ± 6.5
75	8	4.4 ± 0.5	5.0 ± 0.5	5.6 ± 0.4	196.1 ± 14.2	13.8 ± 5.6	195.9 ± 14.2	5.6 ± 0.4	195.8 ± 13.8

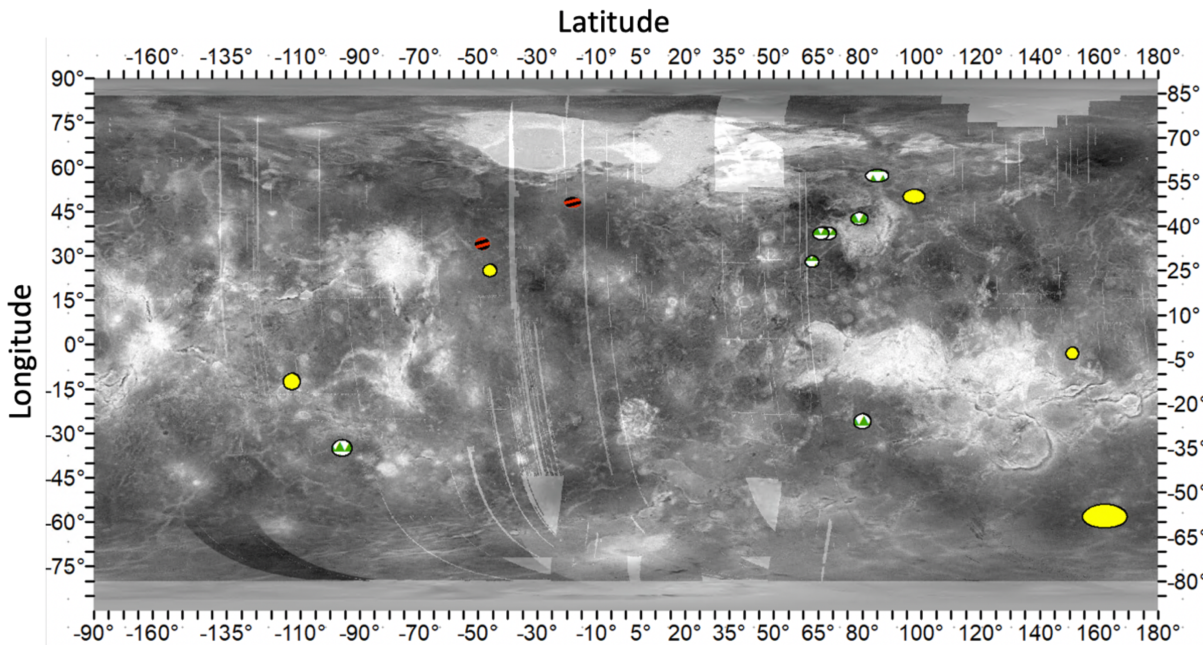

Figure S1. Our derived estimates for elastic thickness generally agree with those derived from admittance data (Anderson & Smrekar, 2006). Ellipses representing domes for which we derived elastic thickness overlay a map of global topography. The ellipses are color and pattern coded based on the agreement between our derived elastic thicknesses and those from a global map constructed from admittance (the ratio of gravity to topography). The size of each ellipse represents the resolution of gravity data at that point. Green triangles, solid yellow, and red striped ovals indicate domes with excellent (>50% within ±20 km), good (>0–50%), and no (0%) agreement, respectively.

Data Set S1. Radar images showing the orientation of all topographic profiles around each dome that were drawn using JMARS. The #1 profile points directly north, and the index numbers increase clockwise as labeled in Figure 2.

Data Set S2. Raw data (elevation versus distance along track) that was extracted from each topographic profile that was amenable to a flexural interpretation. These data were fit to the equations listed in the main text using the curve-fitting algorithm that is included with Matlab.